Synergistic Effect of Benzonitrile and Benzothiazole on the Corrosion Inhibition of 316 Stainless Steel in 6M HCl Solution

Roland Tolulope Loto, Cleophas Akintoye Loto, Alexander McPepple, Gabriel Olanrewaju and Akanji Olaitan

Abstract The synergistic effect of the combined admixture of benzonitrile and benzothiazole (BBZ) on the corrosion inhibition of 316 austenitic stainless steel in 6M HCl solution was evaluated through potentiodynamic polarization, coupon measurement, optical microscopy and IR spectroscopy analysis. Results obtained showed the effective corrosion inhibition performance of the admixture with optimal inhibition efficiency value of 95%. Identified functional groups of alcohols, phenols, amines, amides, carboxylic acids, aliphatic amines, esters and ethers within the compound completely adsorbed onto the steel from analysis of the adsorption spectra while others decreased in intensity due to partial adsorption. Thermodynamic calculations showed the cationic adsorption through chemisorption mechanism according to Langmuir and Freundlich adsorption isotherms. Micro-analytical images showed a badly corroded morphology with corrosion pits in the absence of compounds which contrast the images obtained with the compound. The compound was determined to be mixed type inhibition.

Keywords Corrosion · Inhibitor · Adsorption · Steel

Introduction

Corrosion problems are responsible for a significant percentage of the total costs for most industries worldwide due to the aggressive nature of industrial environments on metallic surfaces of equipment and structures. These problems are associated with operational setbacks, plant shutdowns and equipment maintenance, leading to recurrent partial and even total process shutdown etc. causing in enormous

R. T. Loto (✉) · C. A. Loto · A. McPepple · G. Olanrewaju
Department of Mechanical Engineering, Covenant University, Ota, Ogun State, Nigeria
e-mail: tolu.loto@gmail.com

A. Olaitan
Department of Chemical Metallurgical & Materials Engineering,
Tshwane University of Technology, Pretoria, South Africa

economic losses [1]. Stainless steel corrosion is an electrochemical process, induced by certain electrolytic phenomena in interaction with corrosive environments. These steels are generally corrosion resistant and do perform optimally, however the limit of their corrosion resistance depends on the composition of operating environment and strength of their passive protective films which itself is a product of the alloy composition and metallurgical structure. The continuous exposure of stainless steels to action of acids results in accelerated deterioration of the steels due to breakage of the passive film at specific sites through which aggressive ions penetrate and initiate corrosion in the form of localized attacks [2–4]. Appropriate application of chemical compounds for corrosion inhibition significantly reduces the corrosion effect on the steels [5, 6]. Organic compounds containing heteroatoms in their structure tends to be effective inhibitors as such this study focuses on the synergistic corrosion inhibition properties of benzonitrile and benzothiazole on 316 austenitic stainless steel.

Experimental Procedure

316 austenitic stainless steel (316SS) obtained commercially have a nominal composition shown in Table 1. The steel specimens were machined and abraded with silicon carbide papers before cleansing with distilled water and acetone for weight loss analysis. Measured 316SS specimens were separately immersed in 200 mL of 6M HCl solution for 456 h and weighed 24 h to determine the weight loss and corrosion rate. Potentiodynamic polarization test was performed after mounting the steel specimens in epoxy resin (exposed surface area, 1.33 cm^2) with a three electrode system, glass cell with the electrolyte solution and Digi-Ivy 2311 at a scan rate of 0.0015 V/s between potentials of −0.5 V and +1.5 V to obtain the corrosion rate, corrosion current density, corrosion potential, polarization resistance and inhibition efficiency using the Tafel extrapolation method. Spectral patterns of BBZ/6M HCl solution (before and after the corrosion test) was evaluated and equated to the theoretical IR absorption table to identify the functional groups involved in the corrosion inhibition reactions after exposure to specific range of infrared ray beams from Bruker Alpha FTIR spectrometer between wavelengths of 375–7500 cm^{-1} and resolution of 0.9 cm^{-1}. The inhibiting compounds (benzonitrile and benzothiazole) were purchased from BOC Chemical, USA in the synthesized form.

Table 1 Percentage nominal composition of 304LSS and 316SS

Element symbol	Si	N	Ni	Mo	Cr	Mn	P	S	C	Fe
% composition (316SS)	0.75	0.1	11	3	18	2	0.045	0.03	0.08	65

Results and Discussion

Polarization Studies

The corrosion polarization behaviour of 316SS in 0–1.5% BBZ/6M HCl solution is shown in Fig. 1. Results obtained from the polarization test are presented in Table 2. At 0% BBZ, 316SS severely deteriorated at corrosion rate value of 9.91 mm/year, corresponding to a corrosion potential value of 0.316 V. Addition of BBZ compound (0.25–1.5% BBZ) altered the electrochemical behaviour of 316SS due to the effective inhibiting action of BBZ molecules in counteracting the action of Cl^- ions on the stainless steel surface. The current density reduced sharply after 0% BBZ while the corrosion potential value of 316SS at 0.25% BBZ shifted to a less negative value of 0.231 V signifying anodic inhibition, before alternating within specific ranges at higher BBZ concentration due to the mixed inhibiting properties of BBZ through surface coverage resulting from chemisorption reaction mechanisms. The inhibition efficiency values at from 0.25 to 1.5% are significantly above 90%, which is proportional to the high polarization resistance values. The corrosion rate and corrosion inhibition efficiency results (Table 2) shows changes in BBZ concentration is independent of the corrosion rate results, hence is effective at all concentration studied. The maximum change in corrosion potential value for BBZ corrosion inhibition is 85 mV in the anodic direction thus it is an anodic type inhibitor.
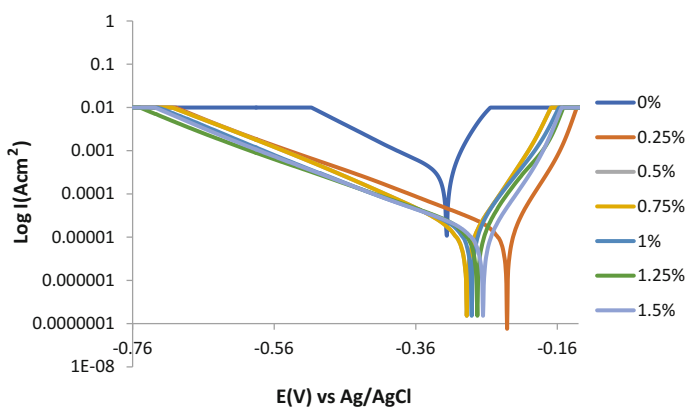

Fig. 1 Potentiodynamic polarization curves for BBZ inhibition of 316SS corrosion in 0–1.5% BBZ/6M HCl solution

Table 2 Potentiodynamic polarization results for BBZ inhibition of 316SS corrosion in 0–1.5% BBZ/6M HCl solution

| Sample	BBZ concentration (%)	Corrosion rate (mm/year)	Corrosion current (A)	Corrosion current density (A/cm^2)	Corrosion potential (V)	Polarization resistance, R_p (Ω)	Cathodic Tafel slope, B_c (V/dec)	Anodic Tafel slope, B_a (V/dec)	Inhibition efficiency (%)
0	0	9.91	7.63E–04	9.65E–04	–0.316	33.70	–7.75	0.04	0
1	0.25	0.35	2.67E–05	3.38E–05	–0.231	962.00	–6.32	34.60	96.50
2	0.5	0.27	2.11E–05	2.67E–05	–0.288	1220.00	–7.82	25.30	97.23
3	0.75	0.29	2.24E–05	2.83E–05	–0.254	1150.00	–4.81	31.60	97.06
4	1	0.35	2.69E–05	3.40E–05	–0.281	956.00	–5.87	21.10	96.47
5	1.25	0.30	2.34E–05	2.97E–05	–0.273	1100.00	–6.08	18.80	96.93
6	1.5	0.26	1.99E–05	2.52E–05	–0.265	1290.00	–6.07	28.80	97.39
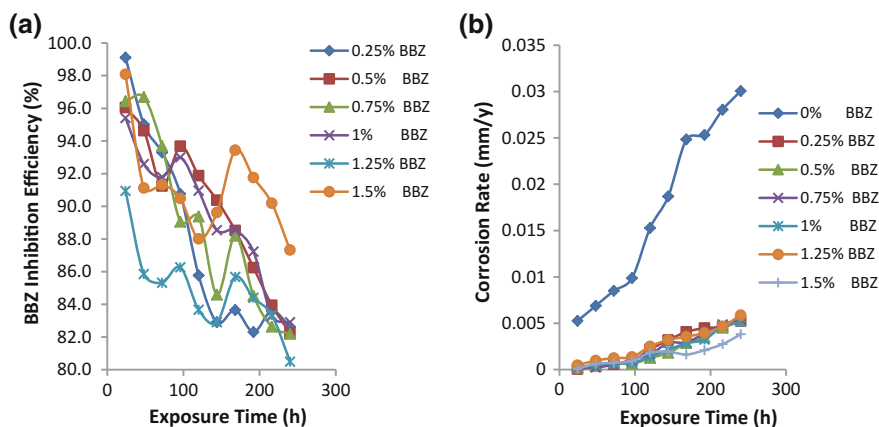
Fig. 2 Graphical plot of **a** BBZ inhibition efficiency, **b** 316SS corrosion rate versus exposure time

Weight-Loss Measurements

Figure 2a, b shows the graphical illustration of BBZ inhibition efficiency and 316SS corrosion rate versus exposure time in the acid media. There is a general decrease in inhibition efficiency corresponding to an increase in corrosion rate during the exposure hours however the corrosion rate of 316SS at 0% BBZ increase exponentially significantly differing from the steel specimens with at specific BBZ concentrations. BBZ compound displayed similar corrosion inhibition characteristics on the corrosion behaviour of 316SS with time basically through adsorption. Its presence in the acid media stifled the oxygen reduction, hydrogen evolution and oxidation reaction mechanism responsible for corrosion. Adsorption of BBZ probably blocked the active sites where the dissolution and release of metal cations into the solution occurs as a result of the action of chloride anions. BBZ belongs to the group of organic compounds consisting of electron rich heteroatoms which are centers of Lewis acid-base interaction with the steel [7]. They act by forming a protective film over the entire exposed area of the steel. The film chemisorbs onto the steel inhibiting the reaction of corrosive anions with the steel [8]. This prevents the passage of metallic cations consisting of Fe^{2+} into the solution.

Adsorption Isotherm

Langmuir and Frumkin adsorption isotherm was applied to describe the adsorption mechanism of BBZ inhibition of 316SS corrosion in 6M HCl solution, as they best fits the experimental results. The negligible deviation of the slopes from unity in Fig. 3a, b is attributed to the molecular interaction among the adsorbed inhibitor
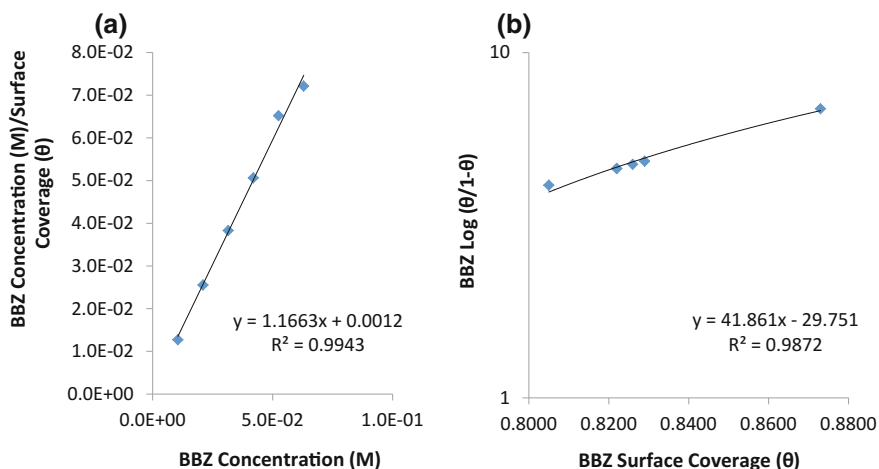
Fig. 3 Adsorption isotherm plots of BBZ adsorption on 316SS surface **a** Langmuir isotherm, **b** Frumkin isotherm

species on the steel surface and changes in the values of Gibbs free energy of adsorption due to changes in surface coverage values. Langmuir isotherm suggests monolayer layer adsorption at specific reaction sites on the steel's surfaces. The adsorptions are identical, equivalent and no lateral interaction between the adsorbed molecules exists [9]. Plots of $\frac{C_{BBZ}}{\theta}$ versus C_{BBZ} (Fig. 3a) perfectly fits with Langmuir isotherm with a correlation coefficient of 0.9943. The Frumkin adsorption isotherm suggests that the steel surface is heterogeneous i.e. lateral interaction effect is not negligible [10]. Plots of $\log\left[\theta/(1-\theta)_C\right]$ versus θ in Fig. 3b showed a correlation coefficient of 0.9872.

Thermodynamics of the Corrosion Process

Results shown in Table 3 give supporting evidence of slight deviation from ideal condition of Langmuir and Frumkin isotherm models due to the differential values of Gibbs free energy of adsorption (ΔG_{ads}) with changes in surface coverage (θ) values. The negative ΔG_{ads} values are due to the spontaneity of the adsorption process as a result of the non-homogeneous nature of the steel surface. The values of ΔG_{ads} calculated ranges between -38.70 and -42.22 kJ mol^{-1} indicating chemisorption adsorption mechanism through electrostatic attraction and covalent interaction and bonding.

Table 3 Data obtained for Gibbs free energy, surface coverage and equilibrium constant of adsorption at specific molar concentrations of BBZ

Samples	LCN conc. (M)	Surface coverage (θ)	Equilibrium constant of adsorption (K)	Gibbs free energy, ΔG (KJ mol^{-1})
A	0	0	0	0
B	1.05E−02	0.826	452306.2	−42.22
C	2.10E−02	0.822	220000.4	−40.44
D	3.15E−02	0.822	146667.0	−39.43
E	4.20E−02	0.829	115478.2	−38.84
F	5.25E−02	0.805	78667.1	−37.89
G	6.30E−02	0.873	109159.4	−38.70

ATF-FTIR Spectroscopy Analysis

The spectra diagram for BBZ adsorption and corrosion inhibition of 316SS in 6M HCl is shown in Fig. 4. Peak configuration of BBZ/6M HCl plot (after corrosion) showed significant decrease in wavelength values between 928.04 and 3065.60 cm^{-1} in comparison to the peak configuration of BBZ/6M HCl plot (before corrosion) due to adsorption of the functional groups (identified through comparison of the wavelength numbers within the range of decreased transmittance with the theoretical table of characteristic IR absorptions) on 316SS during the corrosion inhibition process.
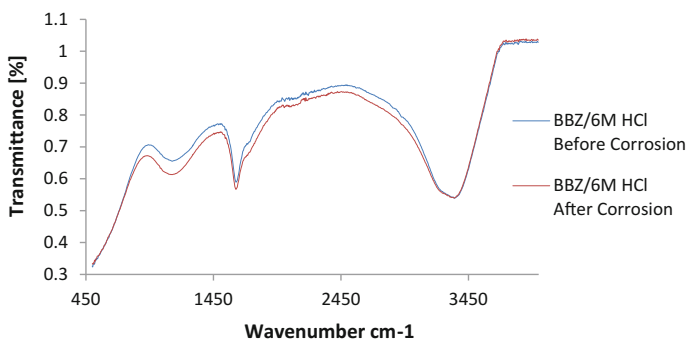
Fig. 4 ATF-FTIR spectra of BBZ adsorption on 316SS 6M HCl solution

Conclusion

BBZ performed effectively in the acid media inhibiting the corrosion of 316 stainless steel. The corrosion inhibition efficiency values of the compound remained generally the same at the concentrations studied with slight deviations as a result of the inhibition reaction of the molecular functional groups and heteroatoms of the compound which influenced the mechanism of the redox electrochemical reactions. Thermodynamic calculations confirm strong chemisorption reaction mechanism and the adsorption aligned with the Langmuir and Frumkin adsorption isotherm. Infrared spectra images confirmed the adsorption of the functional groups resulting in the effective passivation of the steel.

References

1. Garcia-Arriaga V, Alvarez-Ramirez J, Amaya Sosa ME (2010) H_2S and O_2 influence on the corrosion of carbon steel immersed in a solution containing 3M diethanolamine. Corros Sci 52 (7):2268–2279
2. Williams DE, Kilburn R, Cliff J, Waterhouse GIN (2010) Composition changes around sulphide inclusions in stainless steels, and implications for the initiation of pitting corrosion. Corros Sci 52(11):3702–3716
3. Williams DE, Stewart J, Balkwill PH (1994) The nucleation, growth and stability of micropits in stainless steel. Corros Sci 36(7):1213–1235
4. Paroni ASM, Alonso-Falleiros Magnabosco R (2006) Sensitization and pitting corrosion resistance of ferritic stainless steel aged at 800 °C. Corrosion 62(11):1039–1046
5. Trabanelli G (1991) Inhibitors—an old remedy for a new challenge. Corrosion 47(6):410–419
6. Ferreira ES, Giancomelli C, Giacomelli FC, Spinelli A (2004) Evaluation of the inhibitor effect of L-ascorbic acid on the corrosion of mild steel. Mater Chem Phys 83:129–134
7. James OO, Ajanaku KO, Ogunniran KO, Ajani OO, Siyanbola TO, John MO (2011) Adsorption behaviour of pyrazolo [3, 4-b] pyridine on corrosion of stainless steel in HCl solution. Trends AppL Sci Res 6(8):910–917
8. Felicia RS, Santhanalakshmi S, Wilson SJ, John AA, Susai R (2004) Bull Elect 20(12): 561–565
9. Guidelli R (1992) Adsorption of molecules at metal electrodes. VCH Publishers lnc., New York, p 1
10. Hosseini M, Mertens SFL, Arshadi MR (2003) Synergism and antagonism in mild steel corrosion inhibition by sodium dodecylbenzenesulphonate and hexamethylenetetramine. Corros Sci 45:1473–1489
11. George S (2004) Infrared and Raman characteristic group frequencies: tables and charts. Wiley, New York